Puffing and Microexplosion Behavior of Water in Pure Diesel Emulsion Droplets During Leidenfrost Effect

Mohammed Yahaya Khan, Z. A. Abdul Karim, A. Rashid A. Aziz, Morgan R. Heikal & Cyril Crua

Taylor & Francis
Taylor & Francis Group

Puffing and Microexplosion Behavior of Water in Pure Diesel Emulsion Droplets During Leidenfrost Effect

Mohammed Yahaya Khan [iD][a], Z. A. Abdul Karim[a], A. Rashid A. Aziz[a], Morgan R. Heikal[b], and Cyril Crua[b]

[a]Department of Mechanical Engineering, Centre for Automotive Research and Electric Mobility, Universiti Teknologi Petronas, Bandar Seri Iskandar, Malaysia; [b]University of Brighton, School of Computing Engineering and Mathematics, Brighton, UK

ABSTRACT

The microexplosion evolution phenomenon of single droplets of water in pure diesel emulsion under Leidenfrost effect has been studied. The tested emulsions were stabilized with a blend of commercial surfactants with three different water contents of 9%, 12%, and 15%. A high speed camera synchronized with backlight technique was used to capture the evolution of microexplosion and puffing. Three different droplet diameters of approximately 2.6 mm, 2 mm, and 0.2 mm were analyzed. It was found that the tendency of microexplosion and puffing frequency was influenced by the droplet diameter. Coalescence was the dominating factor in inducing microexplosion in bigger droplets. It was observed that the child droplets ejected from the parent droplet undergoes further puffing processes. The size of the secondary droplets after microexplosion were also found to be slightly influenced by the parent droplet size.The waiting time for microexplosion and puffing were compared for different droplets size.

Introduction

In spite of their preferable advantages, diesel engines are one of the foremost pollution contributors to the environment (Basha and Anand, 2011; Brijesh et al., 2015). One way to combat these drawbacks of compression ignition (CI) engines can be overcome by fuel-based solutions, which can be readily adapted to the existing engines without any modifications. Emulsified fuels are considered as one of the conceivable alternative fuels for reducing the engine exhaust emissions (Abu-Zaid, 2004; Armas et al., 2005; Park et al., 2000; Yahaya Khan et al., 2014). The most noticeable effect of such fuels is the secondary atomization occurring during the combustion process. The volatility difference between the base fuel and the dispersed water droplets results in superheating of the water, which is achieved before the base fuel, and rapid vapor expansion, which leads to a violent microexplosion of the emulsified droplets (Watanabe et al., 2010). The presence of water aids to reduce the combustion temperature, therefore reducing NOx. The microexplosion phenomena results in the formation of smaller droplets with a very high surface-to-volume ratio, which results in better mixing with air leading to more complete combustion and lower particulate matter (PM) emissions.

Table 1. Droplet sizes and emulsion fuels on previous studies.

Reference	Emulsion fuels used	Parent droplet diameter (mm)
Ocampo-Barrera et al. (2001)	Heavy fuel oil/water	0.83
Tanaka et al. (2006)	*n*-Dodecane + *n*-tetradecane + *n*-hexadecane + water	2
Watanabe et al. (2009)	Kerosene/water	0.7–1.3
Morozumi and Saito (2010)	*n*-Hexadecane/water	1.5–1.8
Suzuki et al. (2011)	Kerosene/water	0.85–0.99
Tarlet et al. (2014)	Sunflower oil/water	0.15–0.45
Califano et al. (2014)	Commercial diesel/water	0.7–1.1
Mura et al. (2014)	Sunflower oil/water	1

The microexplosion phenomenon is often quoted for countering the engine exhaust emissions (i.e., reducing PM and NO_x simultaneously). Therefore, understanding the microexplosion phenomena can help to increase the efficiency of alternative fuels, in particular with water in diesel emulsions. Usage of suspended droplets on thermocouple or quartz fiber has been studied previously to record the temperature history of the heated emulsion droplets, i.e., emulsion of pyrolysis oil in diesel oil (Calabria et al., 2007), *n*-dodecane and *n*-tetradecane in water emulsion (Tsue et al., 1996), kerosene and water emulsion (Watanabe et al., 2009), commercial diesel and water emulsion (Califano et al., 2014), and diesel-bio diesel-ethanol blends (Avulapati et al., 2016). One of the main demerits in these type of techniques is that the presence of thermocouple or the fiber wire results in the heterogeneous bubble nucleation on the surface of the wire (Watanabe et al., 2010). A 50-μm-diameter R-type thermocouple was used in their study. On the other hand, Mura et al. (2014) concluded that the presence of 76.2-μm-diameter K-type thermocouple did not dominate the microexplosion process. However, the size, geometry, and heat transfer to the thermocouple from the droplet and its effect on the microexplosion evolution is still unclear.

Also, prior studies confirmed that the microexplosion does not always occur (Califano et al., 2014; Khan et al., 2014; Yahaya Khan et al., 2016). The droplet diameters considered for the purpose of visualization of the microexplosion evolution were different among the studies. Emulsion fuels with the parent droplet size, studied previously by the other researchers for the development of microexplosion phenomenon, are highlighted in Table 1. This experimental work investigates the evolution of microexplosion phenomenon of water in pure diesel emulsion droplets. Breakup characterization studies of child droplets are scarce and are limited to base fuels other than pure diesel (Avulapati et al., 2016). Such characteristics are also studied here by analyzing the primary and secondary droplet sizes in order to fill in this gap in the knowledge base. The droplet sizes studied in this experiment are within the comparable range of other researchers, so as to compare the present results with their works.

Materials and methods

Emulsion preparation and stability

The water in diesel emulsions (WiDE) used in this study was blended at 1500 rpm for 15 min using an overhead stirrer. Mixtures of commercial surfactants, Span-80 with a hydrophilic-lipophilic balance (HLB) value of 4.3 and an HLB of 11 for TWEEN 85, were used as emulsifiers. Surfactants are necessary to lower the interfacial tension between the diesel and water to form a stable emulsion. The base fuel used was pure diesel without any additives. The emulsions were stabilized with 15% of surfactant concentration to the water content. The

Table 2. The preparation matrix for the WiDE.

Volume of surfactant	Sample ID	Amount of H_2O (ml)	Volume (ml)	
15% from H_2O			Diesel	Surfactant
	WiDE-1	9	89.65	1.35
	WiDE-2	12	86.20	1.8
	WiDE-3	15	82.75	2.25

preparation matrix for the WiDE is shown in Table 2. All of the prepared emulsions were found to be stable for almost 30 days. This was due to the dosage of surfactant blend being sufficient to the overall surface of the dispersed compound to be completely covered by the surfactant molecules (Abdul Karim et al., 2014).

An HLB value of 9 was used for stabilizing all the emulsions. It was obtained by mixing the two surfactants by the following equation:

$$\% A = 100 * \frac{\times - HLB_B}{(HLB_A - HLB_B)} \tag{1}$$

where HLB_A = HLB value of surfactant A; HLB_B = HLB value of surfactant B; x = required HLB value; $\% A$ = Quantity of surfactant A required; $\% B$ = quantity of surfactant B required ($\% B = 100 - \% A$).

Experimental setup

Schematic diagram of the experimental setup for the evolution of microexplosion visualization is shown in Figure 1. The basic principle of the setup is the same as that of Mura et al. (2012). A PHANTOM MIRO M310 high speed camera was used for image capturing. The image acquisition rate was set at 8000 fps for larger droplets and 10,000 fps with a resolution of 640 × 480 for droplets with the smallest diameter. A polished flat aluminum plate with a small concave dent was used to place the droplet; the base plate temperature was maintained at 500 ± 2°C using a ceramic heater to obtain the Leidenfrost effect. The temperature was maintained throughout the
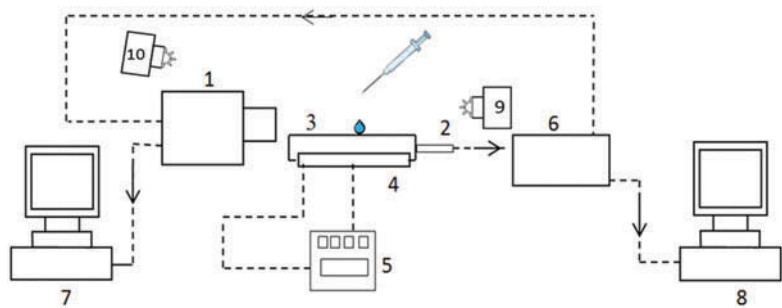
Figure 1. Microexplosion visualization schematic diagram. 1: High speed camera, 2: thermocouple for hot plate, 3: hot plate, 4: ceramic heater, 5: temperature controller for hot plate, 6: N.I. controller, 7 and 8: PC for data acquisition and image processing, 9: light source for backlight illumination, 10: light source for front light illumination.

experiment by a digital temperature controller. The water droplets distribution images were captured by using a digital microscope with a magnification of 1000× and the Sauter mean diameter of dispersed water droplets were calculated by post-processing the images obtained. The light source used for backlight illumination purpose was a single LED type and was synchronized with the exposure time of the high-speed camera. Also, a light source with 12 high power LEDs was used for direct image recording to observe the phase changes and internal features of the droplet during the evolution of microexplosion. The recording speed was set at 2000 fps with a resolution of 510 × 510 pixels. The images were post-processed using the phantom camera control software for measurements and calculating the waiting time of micro-explosion. Approximately 2.6-mm and 2-mm-sized droplets diameters of WiDE were generated using a syringe of 0.8-mm and 0.4-mm orifice diameter needles. Due to the limitations in the generation of smaller droplets, a single bigger emulsion droplet with a diameter of 2.6 mm was made to fall on the heated aluminium plate from a height, which results in immediate shattering of the bigger droplet into numerous smaller droplets with a diameter of approximately 0.2 mm. It should be noted that if the created smaller droplets are not formed of emulsions it will not develop microexplosion. On the other hand, if the droplets are formed only with pure diesel it will not undergo microexplosion phenomenon, instead it will only evaporate (Khan et al., 2014). Each emulsion sample was tested three times under the same testing conditions to ascertain the behavior. The high-speed camera was set to start recording the events as soon as the droplet touched the hot plate. This was achieved by the pre-trigger option available with camera-control software. This facilitated the identification of the exact starting time during post-processing of the captured images.

Results and discussion

The water droplet distribution in the emulsions was captured using a digital microscope with a magnification of 1000× as shown in Figure 2. The water droplet diameter measurements were made using the Motic Image plus 2.0 software.

The sizes of the measured droplets were expressed in terms of Sauter mean diameter (SMD; D_{32}) as follows:

$$D_{32} = \sum\nolimits_i (n_i \times D_i^3) / \sum\nolimits_i (n_i \times D_i^2) \qquad (2)$$

where D_i is the diameter of the droplet and n_i is the total number of droplets having the same diameter. The size distribution of water droplets of the samples are depicted in Figure 3. It is clear from Figure 3 that WiDE-1 had a wide range of distributed water droplet diameters, even with sizes of 7.6 μm to 8.4 μm; whereas WiDE-2 had diameters of
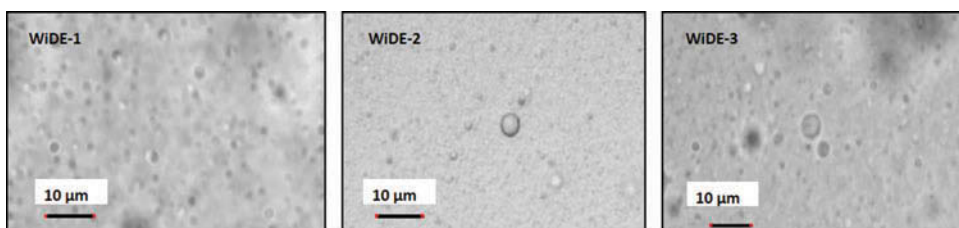
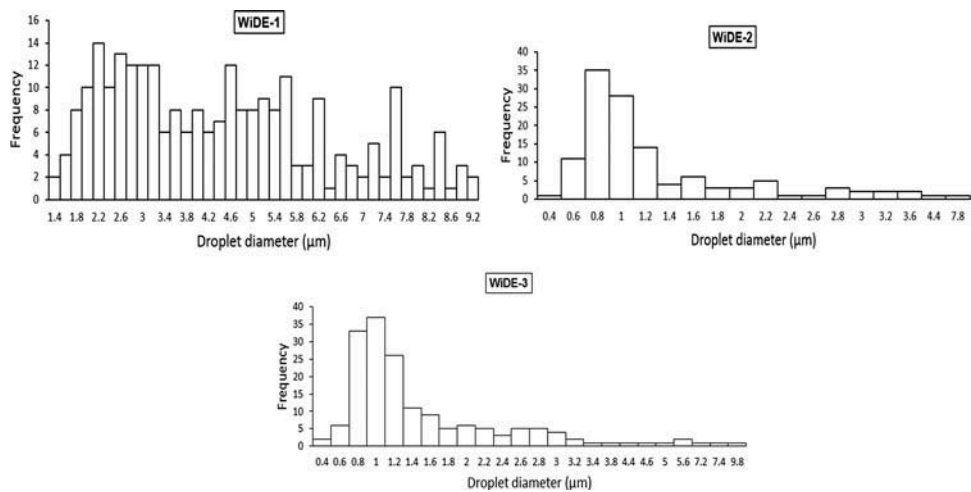**Figure 2.** Images of WiDE, from left to right, with 9%, 12%, and 15% water content, respectively.

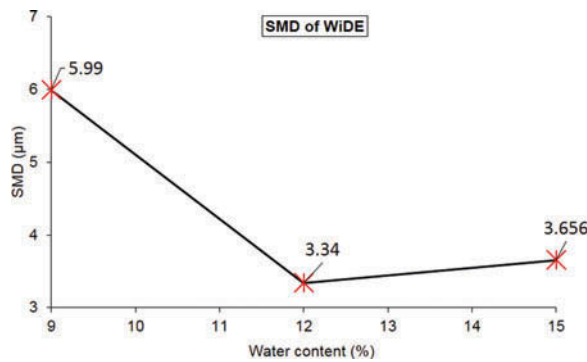Figure 3. The size distribution of water droplets of WiDE samples.

Figure 4. Sauter mean diameter (SMD) of WiDE vs. water content.

0.8 μm to 1.2 μm and WiDE-3 had 0.8-μm to 1.4-μm-diameter droplets, which were more densely populated.

For the same surfactant dosage, the SMD of WiDE-1 was around 6 μm, 3.34 μm for WiDE-2, and 3.65 μm for WiDE-3 as shown in Figure 4. In the case of WiDE-1, an uneven size distribution of wide range of droplet diameters was present, whereas the difference between the droplet diameters for WiDE-2 and WiDE-3 was very small. According to Mura et al. (2012), in his studies on microexplosion of water in sunflower oil, the uneven distribution of bigger droplets leads to faster coalescence and eventually microexplodes.

Physical properties of the prepared emulsions are tabulated in Table 3. The density of the emulsions was found to be almost the same for all of the WiDE samples and the viscosity was increasing with increasing water content. The surface tension of WiDE-1 was lower compared to the other two samples.

Table 3. Physical properties of WiDE.

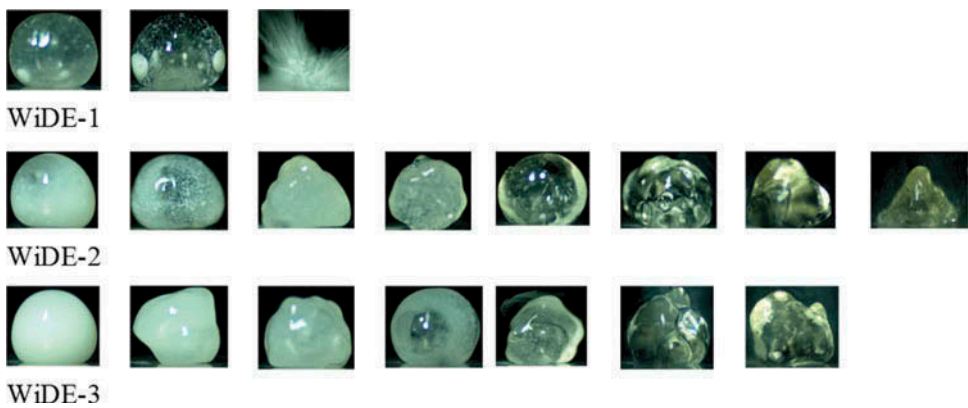| Sample ID	Density @ 20°C (g/m^3)	Viscosity @ 40°C (m pas)	Surface tension @ 20°C (mN/m)
Pure diesel	0.84376	2.7396	—
WiDE-1	0.86109	3.4223	27.47
WiDE-2	0.86052	3.6863	32.27
WiDE-3	0.87140	4.6791	31.11

Figure 5. Evolution of Ø2.6-mm droplets WiDE-1, -2, and -3 at every 0.5-s time interval.

Microexplosion evolution of WiDE with bigger parent droplet

The evolution of WiDE Ø2.6 mm (approximately) size droplets is shown in Figure 5. Since no significant changes in the emulsion phase were observed in the early part of the experiment after the placing of the droplet on the surface, the image sequence shown is from 2 s onward and was captured using the direct image recording.

The rate of coalescence to form larger dispersed water droplets was found to be more dominant (as highlighted in Figure 6) in the emulsion WiDE-1 with 9% water, hence more readily exploded when compared to the other two WiDE samples. The size of the coalescenced water droplets was in the range of 650 μm to 1000 μm for WiDE-1, 69 μm
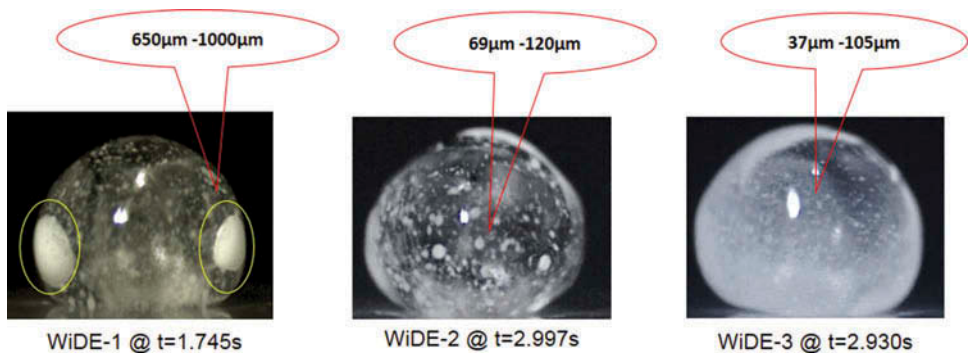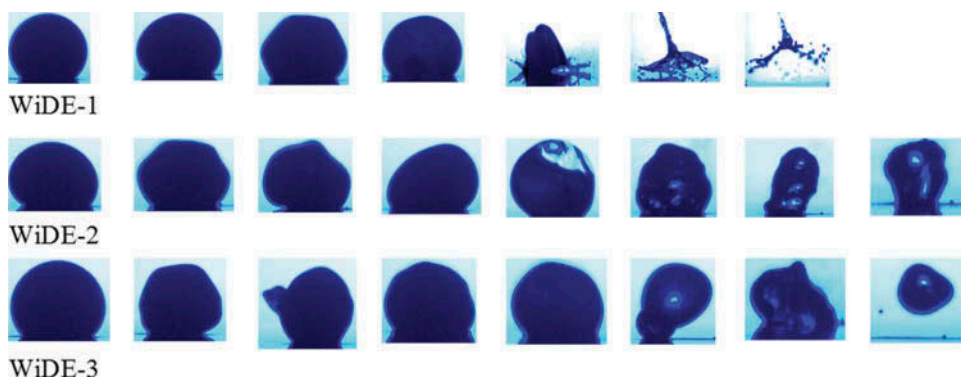

**Figure 6.** Images showing the phase change of emulsions with 9%, 12%, and 15% water content with time interval.

Figure 7. Evolution of Ø2.0-mm droplets WiDE-1, -2, and -3 at every 0.5-s time interval.

to 37 μm for WiDE-2, and it was between 120 μm and 105 μm in the case of WiDE-3. The phase change for all the WiDE with Ø2.6 mm is shown in Figure 6 for selected time interval. It is clear from these images that the coalescence is more dominant in the case of WiDE-1 than the other two emulsions. Also, the coalescence leading to phase change occurred earlier than the other WiDE emulsions. As shown in Figure 3, WiDE-1 contains a wide range of different sized dispersed water droplets compared to the other two WiDE samples. This non-uniform distribution of water droplets led to a higher coalescence rate and hence resulted in microexplosion. Whereas the other two WiDE samples having narrow-sized distributed water droplets, with a minimum difference in the values of the SMD, did not undergo intensive coalescence resulting in only phase change with no microexplosion. Similar behavior was observed for all three trials.

The sequence of evolution of the Ø2.0 mm WiDE droplets is shown in Figure 7. The images shown are from 0 s and with a time interval of 0.5 s. Similar behavior occurred in the case of droplets with Ø2.0 mm (approximately) in which WiDE-1 developed micro-explosion whereas the other two emulsions did not. The secondary droplets after micro-explosion from WiDE-1 are shown in Figure 8. Further observation of the secondary droplets from a Ø2.6-mm parent droplet were around an average size of Ø0.22 mm with a standard deviation of 0.181 and the secondary droplets from the Ø2.0-mm parent droplet were around Ø0.19 mm with a standard deviation of 0.112. From these observations it implies that the size of the secondary droplets is slightly influenced by the size of the parent droplet itself. However, more tests have to be performed to confirm this precisely.

Figures 9 and 10 depict the changes in the diameter of the parent droplet at a half-second time interval. For both cases there were no significant changes in the droplet diameter up to 1.5 s, due to the fact that the droplet might not have had enough heating energy. As the time increased, the droplet diameter started increasing due to vapor expansion inside the droplet. As the pressure built up in the droplet and reached a particular point, water leaves the droplets in a very fine mist (Ochoterena et al., 2010). Puffing is the ejection of the inner content of the emulsified droplet without the complete shattering of the parent droplet. At the end of every puffing (resulting in ejection of larger child droplets) the diameter of the parent droplet dropped and underwent further vapor expansion and its diameter increased
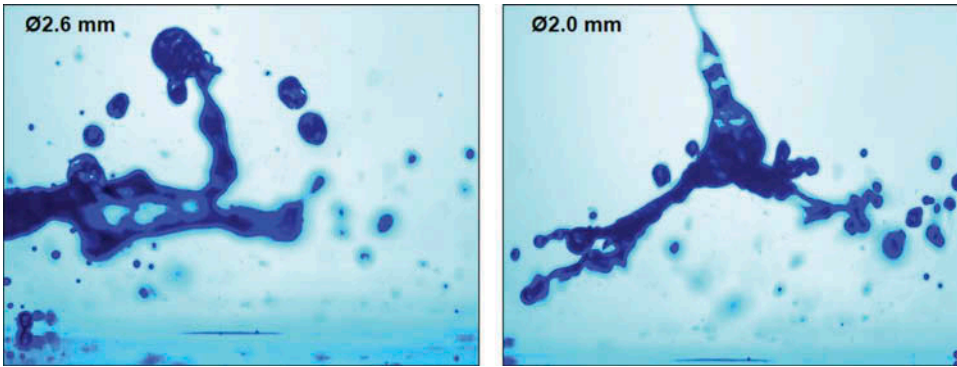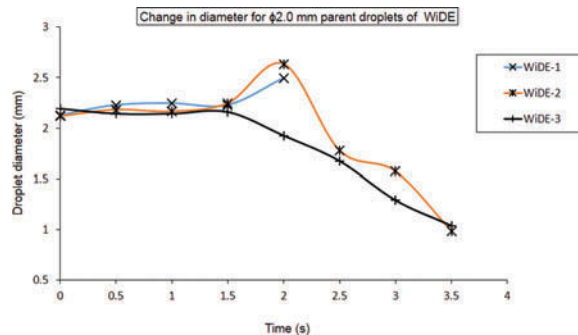
Figure 8. Secondary droplets after microexplosion of Ø2.6-mm and Ø2.0-mm WiDE-1 parent droplets.
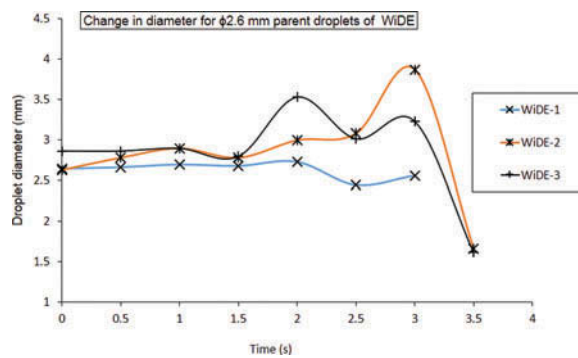

Figure 9. Change in diameter of Ø2.6-mm WiDE droplets at every 0.5-s interval.

Figure 10. Change in diameter of Ø2.0-mm WiDE droplets at every 0.5-s interval.

as shown in the graph. The time taken for initial puffing and the puffing frequency of Ø2.0-mm and Ø2.6-mm WiDE droplets are shown in Figure 11.

The time taken for initial puffing was found to increase with increasing water content in the case of Ø2.6-mm droplet diameter, whereas no such trend was observed in the case of Ø2.0-mm-diameter droplets. However, it is clear from Figure 11 that the time taken for the initial puffing was considerably less in the case of smaller droplet of WiDE.
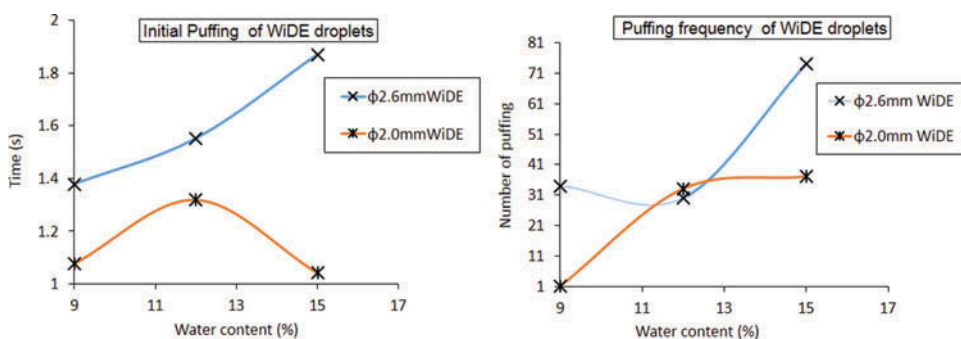
Figure 11. Time taken for initial puffing and the puffing frequency of Ø2.6-mm and Ø2.6-mm WiDE droplets.

Figure 12. Puffing of a child droplet of 0.5681 mm ejected from parent droplet of Ø2.6 mm.

As far as the puffing frequency is concerned, it was comparatively higher for the Ø2.6-mm droplet than the Ø2.0-mm droplet. Notably, WiDE-3 with 15% water content exhibited maximum puffing frequency irrespective of the droplet diameters. It was found that the parent droplet size played an important role in the puffing frequency with the larger parent droplets producing high puffing frequencies.

As highlighted in Figure 12, the child droplets ejected from the parent droplet during puffing were observed to undergo further puffing. The ejected child droplet was about Ø0.568 mm. The child droplet was ejected at 1.590 s from the parent droplet and the puffing time for the child droplet was at 1.5921 s.

Microexplosion and puffing behavior of smaller WiDE droplets

The microexplosion evolutions of the smaller droplets of Ø0.2 mm to Ø0.3 mm are discussed in this section. These droplets were generated by dropping a larger droplet from a height onto the hot plate, which resulted in the production of smaller droplets.
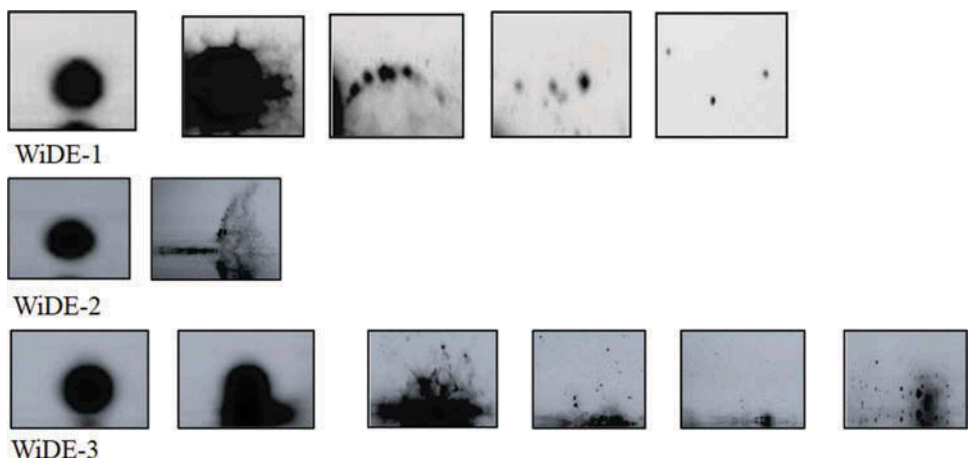
Figure 13. Microexplosion of smaller WiDE droplets.

Table 4. Waiting time of smaller droplets of WiDE.

Sample ID	Droplet diameter (mm)	Microexplosion time (s)	Average diameter of secondary droplets after microexplosion (mm)
WiDE-1	0.17	0.196	0.053
WiDE-2	0.23	0.152	0.031
WiDE-3	0.30	0.233	0.030

Since it was not possible to control the size or the movement of the droplets generated this way, only selected droplets, which underwent microexplosion, were considered for analysis excluding bouncing droplets. These images were captured at 10,000 fps. The microexplosion behavior of smaller droplets of WiDE-1, 2, and 3 are shown in Figure 13.

The waiting times of the parent droplets and the size of the secondary droplets after microexplosion are shown in Table 4. The secondary droplets created after microexplosion of parent droplets were between 1/3 and 1/10 of the size of the parent droplets. Figure 14 shows the instantaneous images of a puffing sequence of WiDE-2, which was observed with the smaller parent droplet of Ø0.2 mm and resulted in child droplets of Ø0.135 mm and Ø0.138 mm. The duration of puffing was 0.002 s. As shown in Figure 14, the diameter of the
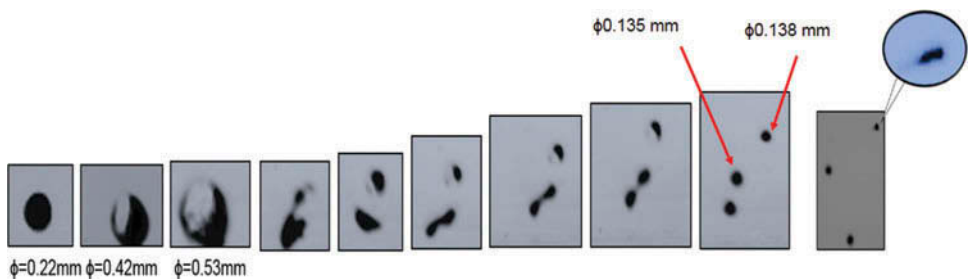

Figure 14. Puffing sequence of a parent droplet of diameter Ø0.224 mm, resulting in ejection of child droplets.

parent droplet increased due to vapor expansion and resulted in the puffing of child droplets. The ejected child droplets were observed to undergo further puffing processes as shown.

Conclusions

WiDE with different parent droplet sizes was visualized for the microexplosion evolution and the outcomes of the observation are summarized as follows:

- Coalescence and the size of the coalescenced water droplet was the dominant factor in inducing the microexplosion phenomenon in the case of large droplets.
- Puffing frequency of the WiDE droplets was found to be a function of the parent droplet size.
- The child droplets ejected during puffing of parent droplets underwent further puffing processes.
- Unlike the large diameter droplets, the small sized (Ø0.2 mm) WiDE droplets developed microexplosion irrespective of their water content.
- The size of the child droplets after microexplosion was almost less than 1/10 of the size of the parent droplet for large droplets (Ø2.6 mm and Ø2.0 mm) and between 1/3 and 1/10 of the size of the smaller parent droplet. The present testing conditions implies that the size of the secondary droplets is slightly influenced by the size of the parent droplet itself. However, further tests have to be performed to confirm this precisely.

ORCID

Mohammed Yahaya Khan 🆔 http://orcid.org/0000-0001-7522-2060

References

Abdul Karim, Z.A., Khan, M.Y., Aziz, A.R.A., and Tan, I.M. 2014. Characterization of water in diesel emulsion. *MATEC Web Conf.*, **13**, 02006.

Abu-Zaid, M. 2004. Performance of single cylinder, direct injection diesel engine using water fuel emulsions. *Energy Convers. Manage.*, **45**, 697–705.

Armas, O., Ballesteros, R., Martos, F., and Agudelo, J. 2005. Characterization of light duty diesel engine pollutant emissions using water-emulsified fuel. *Fuel*, **84**, 1011–1018.

Avulapati, M.M., Ganippa, L.C., Xia, J., and Megaritis, A. 2016. Puffing and micro-explosion of diesel–biodiesel–ethanol blends. *Fuel*, **166**, 59–66.

Basha, J.S., and Anand, R. 2011. An experimental study in a CI engine using nanoadditive blended water–diesel emulsion fuel. *Int. J. Green Energy*, **8**, 332–348.

Brijesh, P., Chowdhury, A., and Sreedhara, S. 2015. Advanced combustion methods for simultaneous reduction of emissions and fuel consumption of compression ignition engines. *Clean Technol. Environ. Pol.*, **17**, 615–625.

Calabria, R., Chiariello, F., and Massoli, P. 2007. Combustion fundamentals of pyrolysis oil based fuels. *Exp. Therm. Fluid Sci.*, **31**, 413–420.

Califano, V., Calabria, R., and Massoli, P. 2014. Experimental evaluation of the effect of emulsion stability on micro-explosion phenomena for water-in-oil emulsions. *Fuel*, **117**, 87–94.

Khan, M.Y., Abdul Karim, Z.A., Aziz, A.R.A., and Tan, I.M. 2014. Experimental investigation of microexplosion occurrence in water in diesel emulsion droplets during the Leidenfrost effect. *Energy Fuels*, **28**, 7079–7084.

Morozumi, Y., and Saito, Y. 2010. Effect of physical properties on microexplosion occurrence in water-in-oil emulsion droplets. *Energy Fuels*, **24**, 1854–1859.

Mura, E., Calabria, R., Califano, V., Massoli, P., and Bellettre, J. 2014. Emulsion droplet micro-explosion: Analysis of two experimental approaches. *Exp. Therm. Fluid Sci.*, **56**, 69–74.

Mura, E., Massoli, P., Josset, C., Loubar, K., and Bellettre, J. 2012. Study of the micro-explosion temperature of water in oil emulsion droplets during the Leidenfrost effect. *Exp. Therm. Fluid Sci.*, **43**, 63–70.

Ocampo-Barrera, R., Villasenor, R., and Diego-Marin, A. 2001. An experimental study of the effect of water content on combustion of heavy fuel oil/water emulsion droplets. *Combust. Flame*, **126**, 1845–1855.

Ochoterena, R., Lif, A., Nydén, M., Andersson, S., and Denbratt, I. 2010. Optical studies of spray development and combustion of water-in-diesel emulsion and microemulsion fuels. *Fuel*, **89**, 122–132.

Park, J., Huh, K., and Park, K. 2000. Experimental study on the combustion characteristics of emulsified diesel in a rapid compression and expansion machine. *J. Auto. Eng.*, **214**, 579–586.

Suzuki, Y., Harada, T., Watanabe, H., Shoji, M., Matsushita, Y., Aoki, H., and Miura, T. 2011. Visualization of aggregation process of dispersed water droplets and the effect of aggregation on secondary atomization of emulsified fuel droplets. *Proc. Combust. Inst.*, **33**, 2063–2070.

Tanaka, H., Kadota, T., Segawa, D., Nakaya, S., and Yamasaki, H. 2006. Effect of ambient pressure on micro-explosion of an emulsion droplet evaporating on a hot surface. *JSME Int. J., Ser. B*, **49**, 1345–1350.

Tarlet, D., Mura, E., Josset, C., Bellettre, J., Allouis, C., and Massoli, P. 2014. Distribution of thermal energy of child-droplets issued from an optimal micro-explosion. *Int. J. Heat Mass Transfer*, **77**, 1043–1054.

Tsue, M., Kadota, T., Segawa, D., and Yamasaki, H. 1996. Statistical analysis of onset of micro-explosion for an emulsion droplet. *Symp. (Int.) Combust.*, **26**, 1629–1635.

Watanabe, H., Harada, T., Matsushita, Y., Aoki, H., and Miura, T. 2009. The characteristics of puffing of the carbonated emulsified fuel. *Int. J. Heat Mass Transfer*, **52**, 3676–3684.

Watanabe, H., Suzuki, Y., Harada, T., Matsushita, Y., Aoki, H., and Miura, T. 2010. An experimental investigation of the breakup characteristics of secondary atomization of emulsified fuel droplet. *Energy*, **35**, 806–813.

Yahaya Khan, M., Abdul Karim, Z., Aziz, A.R.A., and Tan, I.M. 2016. Experimental study on influence of surfactant dosage on micro explosion occurrence in water in diesel emulsion. *Appl. Mech. Mater.*, **819**, 287–291.

Yahaya Khan, M., Abdul Karim, Z., Hagos, F.Y., Aziz, A.R.A., and Tan, I.M. 2014. Current trends in water-in-diesel emulsion as a fuel. *Scientific World J.*, **2014**, 527472.